An anomalous behavior in degraded bulk heterojunction organic solar cells

2011 Phys. Scr. 84 065803

(http://iopscience.iop.org/1402-4896/84/6/065803)

IOP Publishing Physica Scripta

Phys. Scr. **84** (2011) 065803 (5pp) doi:10.1088/0031-8949/84/06/065803

An anomalous behavior in degraded bulk heterojunction organic solar cells

Vinamrita Singh[1], **Swati Arora**[2], **Pankaj Kumar**[3],
Pramod Kumar Bhatnagar[4], **Manoj Arora**[5] **and Ram Pal Tandon**[1]

[1] Department of Physics and Astrophysics, University of Delhi, Delhi 110007, India
[2] Department of Physics, Zakir Husain College, University of Delhi, Delhi 110002, India
[3] National Physical Laboratory, New Delhi 110012, India
[4] Department of Electronic Science, University of Delhi South Campus, Delhi 110021, India
[5] Department of Physics, Ramjas College, University of Delhi, Delhi 110007, India

E-mail: drswatia@yahoo.com

Received 5 July 2011
Accepted for publication 14 October 2011
Published 8 November 2011
Online at stacks.iop.org/PhysScr/84/065803

Abstract

An anomalous behavior—a change in polarity with the passage of time in the bulk heterojunction poly(3-hexylthiophene) (P3HT):6,6-phenylC61 butyric acid methyl ester (PCBM) organic solar cells—is reported here. This work is a continuation of our previous work where the initial degradation of the organic solar cells, freshly prepared up to 4 h, was mainly due to domain formation in the active layer. With the passage of time, the activity at the interfaces starts becoming significant. A decrease of V_{OC} and J_{SC}, leading to a change in polarity, has been reported and explained up to 300 h after fabrication.

PACS numbers: 81.05.ub, 81.05.Lg

(Some figures in this article are in colour only in the electronic version.)

1. Introduction

The low efficiency, short shelf life and poor stability of organic solar cells are the main reasons why these devices have not been commercialized yet. Although the reported efficiency is about 6–8% [1, 2], degradation is the main problem. Therefore, the primary aim is to check the degradation process, and for that purpose it is essential to find the mechanisms responsible for the degradation. A number of researchers have pointed out qualitatively various degradation mechanisms [3–7]. We believe that the rate of degradation and the responsible dominant mechanism are different for different structures, and there is a need to identify them. Life spans of bulk heterojunctions are very likely dominated by the formation of interface states, the rate of interfacial charge transfer and the shift in the Fermi level [8]. In this paper, the interface/surface states and shift in the Fermi level (pseudo Fermi level) [9] are mainly held responsible for the observed degradation.

The properties of the interface between the various layers and electrodes are responsible for shaping the J–V characteristics. It has been reported that the dipole formed at the interface, the work function of the electrodes (anode and cathode) and the energy level (highest occupied molecular orbital (HOMO)–lowest unoccupied molecular orbital (LUMO)) of the organic material contribute significantly to J–V characteristics [10, 11].

Our previous work [12] showed that during the initial degradation (freshly prepared up to 4 h) there is insignificant change in open circuit voltage V_{OC} and a significant change in short circuit current, J_{SC}. This is because of the growth in size of domains, leading to an increase in the surface area and hence a decrease in J_{SC}. When the cells were studied beyond 4 h up to 300 h after fabrication, it was found that there was a significant decrease in both V_{OC} and J_{SC}. The degradation continued and cells showed a change in polarity a few hours after fabrication.

2. Experimental details

Various solar cell structures were prepared on patterned indium tin oxide (ITO) glass (18 Ω sqr^{-1}) using the technique reported in our work [12]. Patterned ITO-coated glass substrates were ultrasonicated in soap solution and cleaned thoroughly with distilled water to remove the soap. The substrates were then cleaned by boiling in acetone for 15 min, followed by similar cleaning in trichloroethylene and isopropanol. The substrates were dried in a vacuum oven at 120 °C for 30 min. Finally, the substrates were exposed to oxygen plasma for 5 min to increase the surface wettability. PEDOT:PSS was spin coated at 2000 rpm for 2 min on the substrates. The samples were annealed at 100 °C for 15 min in a vacuum oven. To prepare the active layer, a solution of poly(3-hexylthiophene) (P3HT):6,6-phenylC61 butyric acid methyl ester (PCBM) (1 : 1 ratio by weight) was taken in chlorobenzene and spin coated at 1000 rpm for 2 min to form a ∼170 nm thick layer. The samples were finally annealed at 120 °C for 15 min. In all these structures, the Al electrodes were thermally evaporated in vacuum of 4×10^{-6} torr. The following structures were fabricated and studied:

S1	Glass/ITO/PEDOT:PSS/ P3HT:PCBM/Al	without LiF
S2	Glass/PEDOT:PSS/P3HT:PCBM/Al	without ITO and without LiF
S3	Glass/ITO/P3HT:PCBM/Al	without PEDOT:PSS and without LiF
S4	Glass/ITO/PEDOT:PSS/ P3HT:PCBM/LiF/Al	with LiF
S5	Glass/PEDOT:PSS/P3HT:PCBM/ LiF/Al	without ITO and with LiF
S6	Glass/ITO/P3HT:PCBM/LiF/Al	without PEDOT:PSS and with LiF

The photovoltaic characterization of all the uncapsulated devices was carried out under illuminated conditions using a solar simulator SS50AAA with 100 mW cm^{-2} power intensity. The organic solar cells were illuminated from the ITO side and current–voltage characteristics were measured using a Keithley 2400 source meter unit. The cells were not under constant illumination and were exposed to light only when the measurements were carried out. The measurements for all the devices were carried out one by one immediately after deposition and then all the devices were stored under the same clean room environmental conditions (under normal atmospheric pressure and temperature). The *J*–*V* measurements on these devices were carried out at regular time intervals up to 300 h after fabrication.

3. Results and discussions

Figures 1(a)–(f) show normalized V_{OC} and J_{SC} with time obtained from figures 1(g) and (h) shown for all the structures. It can be seen that in all the structures both V_{OC} and J_{SC} show a change of polarity with time. For each cell, the time of change in polarity is found to be different for different structures as shown in table 1.

During ageing, the following factors contribute:

- Degradation of electrodes, ITO and Al
- Degradation due to a change in the active polymer layer
- Degradation due to exposure of PEDOT:PSS to moisture
- Degradation due to changes at ITO/PEDOT:PSS, PEDOT:PSS/P3HT:PCBM and P3HT:PCBM/Al interfaces.

The net effect can be physically explained in terms of the following:

- Shifting in HOMO–LUMO level of polymer blend
- Changes in the work function of ITO and Al.

The results are best explained with the help of proposed mechanisms shown schematically in figures 2(a)–(c). Figure 2(a) presents the band diagram of a freshly prepared P3HT:PCBM blend solar cell. Figure 2(b) shows the band diagram after donor–acceptor domain formation sets in during initial degradation, whereas figure 2(c) shows the proposed modified energy levels for long-hour (beyond 40 h) degradation. The degradation may be attributed to a shift in HOMO–LUMO level by introduction/diffusion of impurities such as Al and In or their corresponding cations [13, 14], molecules of O_2 and H_2O [4]. We believe that the interlayer formation at various interfaces introduces interface states, resulting in a change in HOMO–LUMO of the active layer and the work function of electrodes. The interface states may also be introduced due to other factors such as (i) moisture/oxygen, (ii) chemical reaction at the interface and (iii) impurities. The shift of various energy levels, upward or downward, depends on the interface and the interfacial dipole changes [10]. The change in Al work function to −3.3 eV is approximately the same as that reported by Toyoshima *et al* [9]. The work function of ITO can vary from −4.3 to −5.1 depending on the stoichiometry, organic contamination and oxidation type [15], and we have assumed it to be shifting to about −5.0 eV and this explains our experimental behavior. Further, approximate changes in HOMO–LUMO levels in the active material have been shown in figure 2(c). It is clear from figure 2(c) that there is a good probability of movement of hole from modified P3HT HOMO (−5 eV) to a pseudo work function level of Al (−3.3 eV). The origin of the pseudo work function is the introduction of interface states generated through chemical interaction between active material and the electrode [9]. Similarly, on the other hand, the electrons have a probability to reach ITO through PEDOT:PSS. Under this situation the Al electrode will become positive and the ITO electrode will become negative, i.e. a change of polarity with time. The situation in figure 2(c) will arrive at different times for different structures, depending on the nature of active layer/interface and therefore the time of change of polarity will also vary as shown in table 1. As an example of S1 (without LiF) the degradation is very slow but when the structure is modified by putting LiF (S4) between the active layer and aluminum, the current improves slightly but the cell degrades fast, leading to a change in polarity after about 170 h after fabrication. This may be attributed to the fast degradation of LiF/Al electrode. The same argument can be given for S2 and S5 that are without ITO. The cells without ITO are not good because the current density is very small. Here also the change in polarity can be explained on the basis of figure 2(c) discussed above. Similarly, in S3 and S6 the degradation is very fast, because of which the situation shown in figure 2(c) is reached very fast (∼40 h). The removal of PEDOT:PSS is not a good choice in making a solar cell

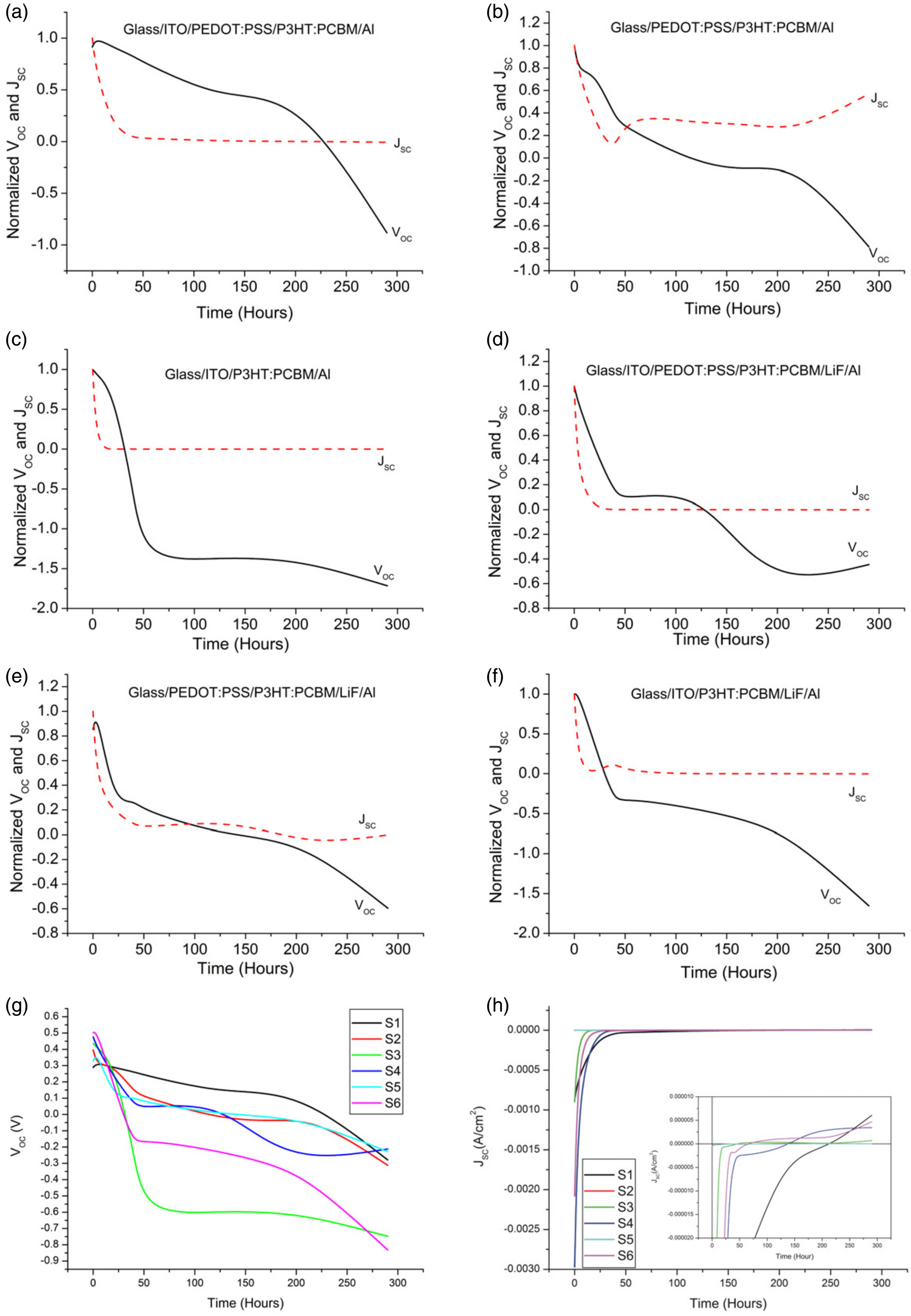

Figure 1. (a) Variation of normalized V_{OC} and J_{SC} for uncapsulated glass/ITO/PEDOT:PSS/P3HT:PCBM/Al as a function of time. (b) Variation of normalized V_{OC} and J_{SC} for uncapsulated glass/PEDOT:PSS/P3HT:PCBM/Al as a function of time. (c) Variation of normalized V_{OC} and J_{SC} for uncapsulated glass/ITO/P3HT:PCBM/Al as a function of time. (d) Variation of normalized V_{OC} and J_{SC} for uncapsulated glass/ITO/PEDOT:PSS/P3HT:PCBM/LiF/Al as a function of time. (e) Variation of normalized V_{OC} and J_{SC} for uncapsulated glass/PEDOT:PSS/P3HT:PCBM/LiF/Al as a function of time. (f) Variation of normalized V_{OC} and J_{SC} for uncapsulated glass/ITO/P3HT:PCBM/LiF/Al as a function of time. (g) Change in V_{OC} with time for the devices. (h) Change in J_{SC} with time for the devices. The inset in the figure shows an enlarged view of the region where a change in polarity takes place.

Table 1. V_{OC} and J_{SC} values for different structures as soon as they are fabricated and after degradation (up to 300 h).

	S1		S2		S3		S4		S5		S6	
Time (h)	V_{OC} (V)	J_{SC} (A cm^{-2})	V_{OC} (V)	J_{SC} (A cm^{-2})	V_{OC} (V)	J_{SC} (A cm^{-2})	V_{OC} (V)	J_{SC} (A cm^{-2})	V_{OC} (V)	J_{SC} (A cm^{-2})	V_{OC} (V)	J_{SC} (A cm^{-2})
0	0.289	−8.72E–4	0.396	−3.05*E*–7	0.436	−8.97E–4	0.476	−2.97E – 3	0.327	−4.86E – 7	0.503	−2.08E–3
4	0.316	−5.77E–4	0.302	−2.32E–7	0.409	−1.45E–6	0.409	−6.96E–4	0.383	−2.01E–7	0.503	−1.66E–4
20	0.289	−1.22E–4	0.302	−9.59E–8	0.315	−6.41E–7	0.235	−2.03E–5	0.1	−9.14E–8	0.182	1.79E–6
40	0.262	−3.23E–5	0.141	−3.35E–9	−0.228	−2.74E–7	0.0605	−2.20E–6	0.107	−4.04E–8	−0.195	−3.44E–6
50	0.242	−2.87E–5	0.107	−1.24E–7	−0.614	3.09E–7	0.0401	−2.62E–6	0.0739	−2.76E–8	−0.144	6.40E–7
120	0.141	−6.34E–6	−0.0204	9.35E–8	−0.597	3.47E–7	0.0738	−1.38E–6	0.00662	−5.28E–8	–	–
170	0.141	−1.75E–6	−0.0435	8.35E–8	−0.597	1.90E–7	−0.181	2.11E–6	−0.0096	1.85E–8	−0.275	1.40E–6
220	0.0570	−6.73E–8	−0.0236	7.10E–8	−0.631	2.82E–8	−0.278	3.27E–6	−0.0555	3.58E–8	−0.430	1.06E–6
290	−0.279	6.05E–6	−0.312	1.74E–8	−0.748	6.75E–7	−0.212	3.44E–6	−0.228	4.04E–10	−0.832	4.67E–6

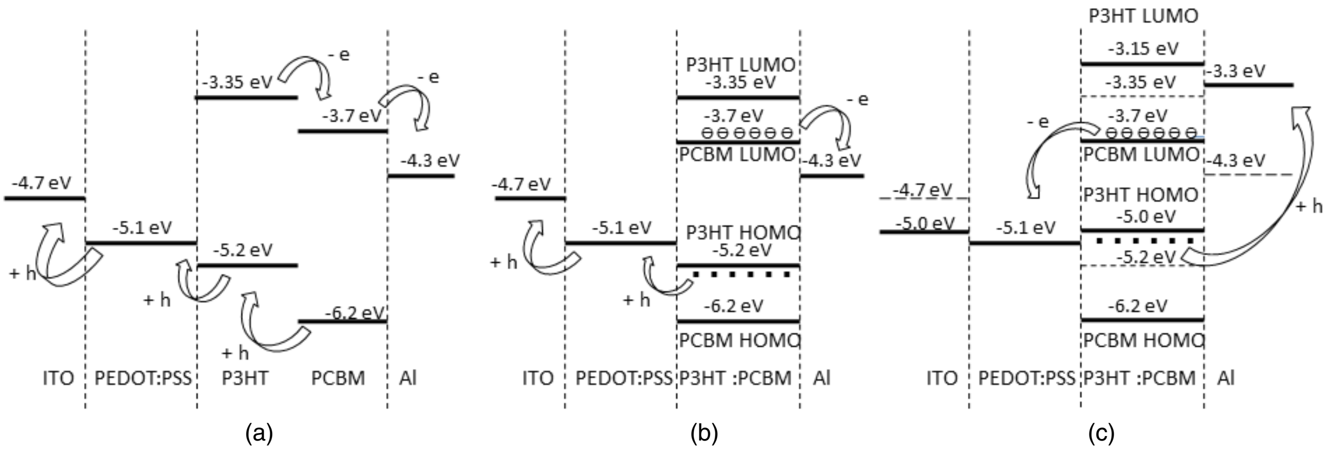

Figure 2. Band diagram of the P3HT:PCBM blend solar cell (a) as soon as it is fabricated, (b) after donor–acceptor domain formation and (c) proposed modified structure after degradation. In panel (c), dotted lines and solid lines represent the energy levels before degradation and after degradation, respectively.

because it helps holes to move. It may be pointed out that just before the change of polarity (where $V_{OC} \approx 0$) there is an equal probability of collecting electrons and holes at the electrodes. In other words, the holes and electrons travel in both directions in the device. In the fresh device the interfaces and barriers at the interfaces enable the net current flow to be in one direction. Upon degradation this balance may tip and cause the net change in polarity as observed.

Attempts can be made to check the cell degradation once the dominant mechanism is known and effective measures can be taken such as proper encapsulation, improved morphology and good electrode contacts. Theoretical calculations are underway to explain the result quantitatively.

4. Conclusion

It can be concluded that the various degradation mechanisms are responsible for the decrease of V_{OC} and J_{SC}, leading to a change in polarity with time as observed by us, and their net effect is to change the energy levels of the donor–acceptor composites and to shift the work functions (pseudo work function) of Al and ITO electrodes. With the passage of time a situation occurs that the direction of carrier collection probability reverses. This leads to a change of polarity of the organic solar cell. There is a need to control the interface states at the surface of the electrode by chemical modification, say by polar species, and shield the diffusion of impurities at the interfaces by adding a densely packed small molecule interlayer.

Acknowledgments

The authors thank DST Purse Grant, India for financial support. We also thank Professor P C Mathur, Department of Electronic Science, South Campus, University of Delhi and Dr M Aslam Parvaiz, Principal, Zakir Husain College, University of Delhi for valuable suggestions and support.

References

[1] Dennler G, Scharber M C and Brabec C J 2009 *Adv. Mater* **21** 1323–38
[2] Lira-Cantu M, Chafiq A, Faissat J, Gonzalez-Valls I and Yu Y 2011 *Sol. Energy Mater. Sol. Cells* **95** 1362–74
[3] Girtan M and Rusu M 2010 *Sol. Energy Mater. Sol. Cells* **94** 446–50
[4] Cai W, Gong X and Cao Y 2010 *Sol. Energy Mater. Sol. Cells* **94** 114–27
[5] Yang H B, Song Cheng Gong Q L and Li C M 2010 *Sol. Energy Mater. Sol. Cells* **94** 846–9
[6] Kumar P, Jain S C, Kumar V, Chand S and Tandon R P 2009 *Appl. Phys.* A **94** 281–6
[7] Jorgensen M, Norrman K and Krebs F C 2008 *Sol. Energy Mater. Sol. Cells* **92** 686–714
[8] Morana M, Koers P, Waldauf C, Koppe M, Muehlbacher D, Denk P, Scharber M, Waller D and Brabec C 2007 *Adv. Funct. Mater.* **17** 3274–83

[9] Toyoshima S, Kuwabara K, Sakurai T, Taima T, Saito K, Kato H and Akimoto K 2007 *Japan. J. Appl. Phys.* **46** 2692–5

[10] Bernede J C, Godoy A, Cattin L, Diaz F R, Morsli M and del Valle M A 2010 *Solar Energy* ed R D Rugescu (Rijeka: InTech) pp 223–61

[11] Street R A, Schoendorf M, Roy A and Lee J H 2010 *Phys. Rev.* B **81** 205307

[12] Arora S, Rajouria S K, Kumar P, Bhatnagar P K, Arora M and Tandon R P 2011 *Phys. Scr.* **83** 035804

[13] Cuiffi J, Benanti T, Nam W J and Fonash S 2010 *Appl. Phys. Lett.* **96** 143307

[14] Krebs F C and Norrman K 2007 *Prog. Photovolt.* **15** 697–712

[15] Centurioni E and Iencinella D 2003 *IEEE Electron Device Lett.* **24** 177–9